Proceedings of the American Control Conference
Anchorage, AK May 8-10, 2002

H-infinity Vehicle Control Using NonDimensional Perturbation Measures

S. Brennan *A. Alleyne**

Dept. of Mechanical & Industrial Engineering

University of Illinois at Urbana-Champaign

1206 W. Green Street, Urbana, IL 61801

**corresponding author*

Abstract

Robust controller design techniques have been applied to the field of vehicle control to achieve many different performance measures: robust yaw rate control [1], robust lateral positioning using one [2, 3] or more [4-6] driver inputs, robust observer design, and so on. A difficulty with many published approaches is to obtain an adequate description of the model uncertainty. Most bounds on plant frequency responses or parameter perturbations are based on ad-hoc limits that rely primarily on the designer's personal choice. The resulting controller design is therefore often vehicle specific, and is suitable only for application to a single design vehicle. This work shows that (a) the description of model uncertainty is not a design variable, (b) meaningful bounds on model uncertainty can be obtained from data and should be sought, and (c) these bounds can be used to generate a single controller suitable for any vehicle.

1. Previous Work and Problem Statement

Previous work [3] presented a robust lateral-position controller useful for highway driving of any passenger vehicle. The system uncertainty was represented as matrix element perturbations of the system matrices. A Linear Matrix Inequality (LMI) approach was then used to design a state-feedback lateral position controller robust to expected parameter variation between vehicles. The resulting controller therefore robustly stabilizes all vehicles dynamically described by the bicycle model and which are parametrically bounded by fixed bounds. Unfortunately, these bounds do not address dynamic uncertainty associated with unmodeled dynamics, disturbances, or measurement noise. An important result of this previous work was the conclusion that a state-feedback controller is not capable of robust lateral vehicle positioning over wide variations in velocity, at least not without some type of gain scheduling.

The controller presented in this work seeks to address controller robustness in a more intuitive framework than previous LMI representations. An H-infinity framework is presented that account for both parametric uncertainty and unmodeled dynamic uncertainty to achieve a robust controller design. A unique aspect of this work is the representation of vehicle dynamics in a nondimensional form that allows a generalized solution to the lateral control problem. Motivating this nondimensional representation is the desire to develop controller implementations suitable to any vehicle, not just a particular research vehicle under study.

This paper is summarized as follows: Section 2 presents equations for the linear, lateral vehicle dynamics with a fixed preview distance. These equations are presented in both dimensional and nondimensional form, with the nondimensional form governed by a new set of unitless parameter groupings known as Π groups. Distributions of these Π groups define an average vehicle dynamic. Section 3 defines the robustness criteria required for generalized vehicle control: that a controller must stabilize the average vehicle dynamics in the presence of perturbations that generate the range of published vehicle dynamics. This range is numerically defined by bounding the frequency-response difference between the average vehicle and 50 other published vehicle dynamics. It was again found that no single controller is capable of robust control over large variations in speed or friction. Section 4 fixes the speed and friction, then develops a robust controller design to demonstrate a single-velocity robust controller implementation. Section 5 then discusses gain-scheduling approaches and limitations to robust control. Finally, a conclusion summarizes the primary results.

2. Vehicle Dynamics

Motivating the nondimensional representation is the desire to develop controller implementations suitable to any vehicle. Consequently, vehicle-to-vehicle variation is addressed in a nondimensional framework that utilizes the Buckingham Pi theorem [7]. The resulting representation accommodates two modeling aspects previously ignored by other researchers: first, parameter-to-parameter interdependency clearly arises due to common vehicle design; second, the individual parameter distributions show a normal distributions in the nondimensional representation, which specifically define a mean and standard deviation of vehicle dynamics [3, 8].

Application of the Buckingham Pi theorem [7] to the classical vehicle dynamics known as the Bicycle Model yields groupings of parameters that collectively do not have dimensions. These dimensionless parameters are known as Π groups, and for the planar bicycle model these parameters are:

$$\Pi_1 = \frac{a}{L}, \Pi_2 = \frac{b}{L}, \Pi_3 = \frac{C_{af} L}{mU^2}, \Pi_4 = \frac{C_{ar} L}{mU^2}, \Pi_5 = \frac{Iz}{mL^2}. \quad (1)$$

With:

m = vehicle mass	(5.451 kg)
I_z = vehicle moment of inertia	(0.1615 kgm^2)
V = vehicle longitudinal velocity	(3.0 m/s)
a = distance from C.G. to front axle	(0.1461 m)
b = distance from C.G. to rear axle	(0.2191 m)
L = vehicle length, a + b	(0.3652 m)
C_{af} = cornering stiffness of front 2 tires	(65 N/rad)
C_{ar} = cornering stiffness of rear 2 tires	(110 N/rad)

The values in parenthesis are quite different from a typical full-sized vehicle because they correspond to the measured values for a 1/7-scale experimental scale used on the Illinois Roadway Simulator, a treadmill/vehicle counterpart to a wind tunnel/airplane testing system. The similarity in dynamics between this vehicle and full-sized vehicles was proven via the Buckingham-Pi Theorem, and was the original motivation for analyzing vehicle dynamics in a nondimensional framework. Derivation and explanations of the vehicle Π parameters are given in more detail in [8].

The Π values of Equation (1) are readily available for many vehicles by utilizing parameters published in the literature for the standard bicycle model; thus far 50 sets of parameters have been recorded in data set hereafter referred to a **V**. Each set member will be referred to as $\mathbf{V_i}$. A relative distribution of vehicle Π parameters for **V** is shown in Fig. 1, with each vehicle traveling at 28 m/s (63 mph). Clearly, a vehicle model described by nondimensional parameters has reduced parametric dimension, from 8 dimensional parameters to 5 nondimensional parameters. Further, Π_2 is not independent and can be obtained by definition:

$$\Pi_2 = 1 - \Pi_1 \quad (2)$$

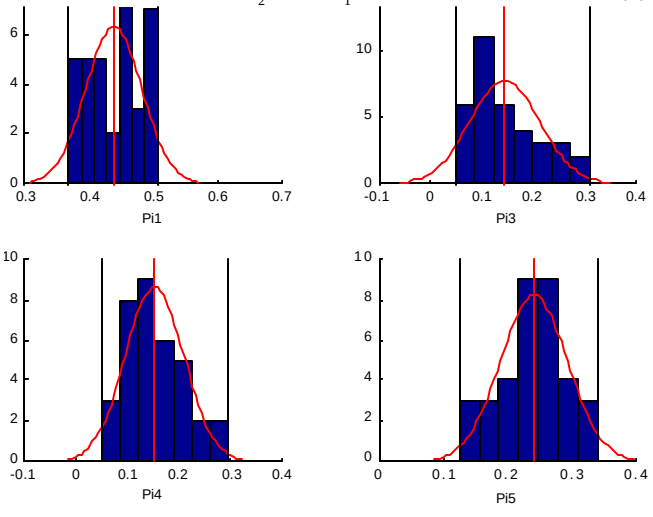

Fig. 1: Distribution of Pi parameters

For this reason, Π_2 is not plotted. From these distributions, the average Π parameters are obtained:

$$\overline{\Pi}_1 = 0.4373, \overline{\Pi}_3 = 0.1534, \overline{\Pi}_4 = 0.1725, \overline{\Pi}_5 = 0.2341 \quad (3)$$

Note that Π_3 and Π_4 are dependent on velocity and cornering stiffness, so these average values change with chosen operating speed and road surface, with ratios given by Equation (1).

The space description of vehicle dynamics is based on the bicycle model [9] with the state vector [lateral position, lateral velocity, yaw angle, yaw rate]:

$$\mathbf{x} \equiv \begin{bmatrix} y & \frac{dy}{dt} & y & \frac{dy}{dt} \end{bmatrix}^T \quad (4)$$

and front steering input, $\mathbf{u} \equiv \begin{bmatrix} d_f \end{bmatrix}^T$, as the sole control channel. Note that all states are measured with respect to the vehicle's center-of-gravity. The state space representation (in path error coordinates) is:

$$\frac{d\mathbf{x}}{dt} = \mathbf{A} \cdot \mathbf{x} + \mathbf{B} \cdot \mathbf{u}, \mathbf{y} = \mathbf{C} \cdot \mathbf{x} \quad (5)$$

with:

$$\mathbf{A} = \begin{bmatrix} 0 & 1 & 0 & 0 \\ 0 & -\frac{f_1}{mU} & \frac{f_1}{m} & \frac{-f_2}{mU} \\ 0 & 0 & 0 & 1 \\ 0 & \frac{-f_2}{I_z \cdot U} & \frac{f_2}{I_z} & \frac{-f_3}{I_z \cdot U} \end{bmatrix}, \mathbf{B} = \begin{bmatrix} 0 \\ \frac{C_{af}}{m} \\ 0 \\ \frac{a \cdot C_{af}}{I_z} \end{bmatrix}, \mathbf{C} = \begin{bmatrix} 1 \\ 0 \\ 0 \\ 0 \end{bmatrix}^T \quad (6)$$

$$f_1 = C_{af} + C_{ar}, f_2 = a \cdot C_{af} - b \cdot C_{ar}, f_3 = a^2 \cdot C_{af} + b^2 \cdot C_{ar}$$

The non-dimensionalization transforms are obtained by a state substitution that normalizes each state with respect to distance, mass, and time. The same approach was used to generate the parameters of Equation (1), and not surprisingly the nondimensional dynamics can be rewritten entirely in terms of the same Π parameters. Mathematically, this is shown via a variable substitution defined by:

$$\mathbf{x} = \mathbf{M} \cdot \mathbf{x}^* \quad (7)$$

The above state normalizations are combined with a time normalization, $t = \mathbf{S} \cdot t^*$. For the vehicle system, $\mathbf{S} = \frac{L}{U}$, and **M** is defined as:

$$\mathbf{M} = diag \begin{bmatrix} L & U & 1 & \frac{U}{L} \end{bmatrix} \quad (8)$$

Giving:

$$\mathbf{A}^* = \begin{bmatrix} 0 & 1 & 0 & 0 \\ 0 & -p_1 & p_1 & -p_2 \\ 0 & 0 & 0 & 1 \\ 0 & \frac{-p_2}{\Pi_5} & \frac{p_2}{\Pi_5} & \frac{-p_3}{\Pi_5} \end{bmatrix}, \quad \mathbf{B}^* = \begin{bmatrix} 0 \\ \Pi_3 \\ 0 \\ \frac{\Pi_1 \cdot \Pi_3}{\Pi_5} \end{bmatrix} \quad (9)$$

$$p_1 = \Pi_3 + \Pi_4, p_2 = \Pi_1 \Pi_3 - \Pi_2 \Pi_4, p_3 = \Pi_1^2 \Pi_3 + \Pi_2^2 \Pi_4$$

A similar nondimensionalization can be obtained in the Laplace domain, generating transfer function dynamics solely dependent on the vehicle Π parameters.

In the dimensional form of vehicle dynamics, many authors have noted that additional feedback modifications, such as error preview [10-12] or full-state feedback [3], make the control problem more amenable. In this work, an error preview scheme is utilized, represented by a modification of the **C** matrix as presented in [11]. Specifically:

$$\mathbf{C} = [1 \quad 0 \quad U \cdot Tp \quad 0]. \tag{10}$$

with *Tp* being the preview time. In the linear description, the effect of preview is equivalent to adding yaw angle feedback, and therefore preview is simply a special case of state-feedback.

In the nondimensional form, the **C*** matrix becomes:

$$\mathbf{C}^* = [1 \quad 0 \quad U \cdot Tp / L \quad 0]. \tag{11}$$

with the term:

$$\Pi_6 = U \cdot Tp / L. \tag{12}$$

as a new Π variable. To pick the value of *Tp*, a wide range of preview values were examined. The performance effect of increasing preview was primarily to increase the phase margin deficiency caused by the two free integrators. The robustness effect of increasing preview was to somewhat reduce high-frequency model uncertainty. This is not very helpful since the difficulty with vehicle robustness is a problem governed generally by low-frequency uncertainty. Rather than include preview as an additional unnecessary design varaible, a fixed preview time of 2 seconds was selected and is used hereafter.

To complete the vehicle model description, it is useful to add additional scaling transforms to limit the largest control effort, tracking error, and reference input to all have unity 1-norms. To do this, one uses a variable transformation suggested by [13]. For the vehicle system, reasonable signal norms are:

$$\begin{aligned} u_{max} &= 0.1745[rad] \left(= 10[degrees]\right) \\ e_{max} &= 0.15[m] \left(= 0.5[scalelanes]\right) \\ r_{max} &= 0.15[m] \end{aligned} \tag{13}$$

Which become in the nondimensional space:

$$\begin{aligned} u^*_{max} &= 0.1745[unitless] \\ e^*_{max} &= \frac{e_{max}}{L} = 0.4184[unitless] \\ r^*_{max} &= \frac{r_{max}}{L} = 0.4184[unitless] \end{aligned} \tag{14}$$

With the signals normalized as above, the goal is to maintain an output position within [-1,1], using control inputs bounded by [-1,1], given a reference input that remains within [-1,1].

3. Perturbation Description

As mentioned earlier, the robust controller problem is not solvable if wide variations in longitudinal velocity or road friction are allowed, both of which are completely captured by variations the Π_3 value (assuming Π_4 is a fixed multiple of Π_3). Thus, a fixed Π_3 must be chosen for controller design *and* for uncertainty representation. For this work Π_3 was fixed at 0.5, a value representing a full-sized vehicle on average road surface at 50 mph. Section 5 discusses extending this approach to velocity scheduling.

The goal of this section is to numerically bound the model uncertainty caused by variations in Π parameters. This numerical bound is used afterward for a robust controller design. Whether a controller design is capable of achieving robust performance depends primarily on the measure of the model perturbation. A very poor method of representing plant uncertainty would be to examine frequency-domain perturbations caused by parameter-by-parameter variations [3] because vehicle parameters are highly interdependent. A principal goal of this work is to use a data-driven approach with an appropriate but simple perturbation representation.

A key insight of this work is to utilize the observed variations in Π parameters in database **V** to describe the expected variation of any vehicle controller. The advantage of this approach is that each set of parameters in the database are correctly cross-correlated, thus avoiding the conservatism of one-at-a-time variable manipulation. Additionally, a controller design that is robust to the wide variations in vehicles in **V** should be portable vehicle-to-vehicle.

From the data in database **V**, we compare the relative error between the average vehicle and each individual database member. The frequency-dependent error, e(*jw*), between the average plant and the ith plant is given by:

$$e(jw) = \left| \frac{G\left(jw, \Pi_{1i}, ..., \Pi_{5i}\right) - G\left(jw, \bar{\Pi}_1, ..., \bar{\Pi}_5\right)}{G\left(jw, \bar{\Pi}_1, ..., \bar{\Pi}_5\right)} \right| \tag{15}$$

Where *G(jw)* represents the frequency response of the vehicle bicycle model dependent on the Π parameters. A simple multiplicative uncertainty description is used to describe this system variation, represented in block-diagram form in Fig. 2.

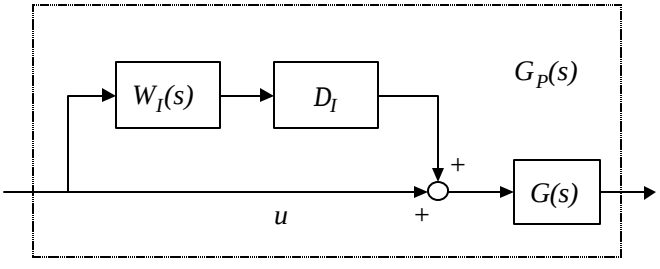

Fig. 2: Multiplicative uncertainty model

The plot of each plant deviation, calculated from (15) for each $\mathbf{V_i}$ in the database **V** is shown in Fig. 3. It is clear that the maximum multiplicative uncertainty is

approximately constant over nearly the entire frequency range, a result that justifies a multiplicative representation.

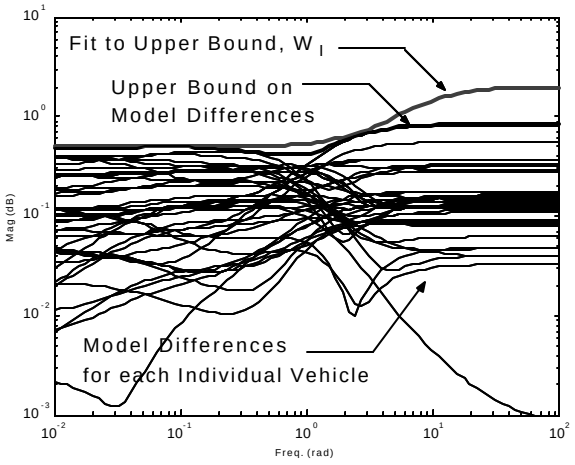

Fig. 3: Multiplicative uncertainty, by frequency

The weight representing system robustness, w_I, is specified by fitting the upper bound of all observed perturbations. In this case:

$$w_I(s^*) = \frac{0.2 \cdot s^* + 0.5}{0.1 \cdot s^* + 1} \tag{16}$$

The high frequency gain was made slightly higher than needed in order to account for possible unmodeled dynamics that are unaccounted for by the bicycle model, such as steering actuator dynamics, vehicle roll and pitch, aerodynamics, etc.

Examining Fig. 3 above, the model uncertainty remains below 1 at low frequencies, up to some crossover point at w* ~ 0.7 rad/sec*. Therefore, the system should be robustly controllable up to this frequency. In the case where the frequency-dependent bound on the uncertainty, w_I, is larger than unity, consider the possible plants that must be controlled. From Fig. 2, we see that in the case that w_I has greater than unit magnitude, a possibility exists that the perturbed plant has zero gain and is for practical purposes uncontrollable. In these situations, no performance can be realized. Such situations arise at very high velocities or low friction values, or at very low values of Π_3. Limiting cases of this phenomenon are discussed in Section 5.

4. Controller Synthesis

With the Π values fixed as above, the nondimensional transfer function for the nominal system is given by:

$$\frac{\overline{y}(s^*)^*}{d_f(s^*)} = \frac{1}{s^{*2}} \frac{19.8 \cdot s^{*2} + 26.08 \cdot s^* + 1.201}{s^{*2} + 2.240 \cdot s^* + 1.6633} \tag{17}$$

Note that $s \Rightarrow s^*$ because s has dimensions of $1/t$ and must also be normalized. With signal normalization as described in Equation (10), the transfer function becomes:

$$\frac{\overline{y}_n(s^*)}{d_f(s^*)} = \frac{\overline{y}^*(s^*)}{d_f(s^*)} \cdot \frac{u^*_{max}}{e^*_{max}} = \frac{1}{s^{*2}} \frac{8.415 \cdot s^{*2} + 11.08 \cdot s^* + 0.5102}{s^{*2} + 2.240 \cdot s^* + 1.6633} \tag{18}$$

Since the H-infinity system representation does not allow unstable open-loop systems, the double integrator is approximated with poles very close to the *jw*-axis:

$$\frac{\overline{y}_n(s^*)}{d_f(s^*)} \approx \frac{1}{(s^* + K)^2} \frac{8.415 \cdot s^{*2} + 11.08 \cdot s^* + 0.5102}{s^{*2} + 2.240 \cdot s^* + 1.6633} \tag{19}$$

with K = 0.0001. The resulting high DC gain approximates the integrator effect.

The H-infinity controller must balance the tradeoff between three frequency domain criteria: performance weighting, represented by $w_P \cdot S$; control effort, represented by $w_u \cdot KS$; and model uncertainty, represented by $w_I \cdot T$. These three design goals are represented approximately by minimization of the stacked H-infinity norm of [13]:

$$\|N\|_\infty = \left\| \begin{matrix} w_P \cdot S \\ w_u \cdot KS \\ w_I \cdot T \end{matrix} \right\|_\infty . \tag{20}$$

While w_I was defined in the previous section, the remaining weights, w_P and w_U, represent design variables. For this problem, these weights were chosen to be :

$$w_P(s^*) = \frac{(1/\sqrt{M_P} \cdot s^* + w_{BP})^2}{(s^* + w_{BP} \cdot \sqrt{A_P})^2} \tag{21}$$

$$w_U(s^*) = \frac{(1/\sqrt{M_U} \cdot s^* + w_{BU})^2}{(s^* + w_{BU} \cdot \sqrt{A_U})^2} \tag{22}$$

Where M_i is the high frequency gain, A_i is the steady-state gain, and w_{Bi} is the approximate crossover bandwidth. The performance weighting function was chosen with M_P = 1.5, with A_P = 0.0001, and w_{BP} = 0.27 rad/sec*. The control weighting was chosen with M_U = 1/100, A_U = 1, and w_{BU} = 100 rad/sec*.

The H-infinity controller is obtained using standard robust synthesis routines, which solve the control problem by iterating through possible controller representations seeking to minimize the norm of Equation (20). A solution was found with a norm of 0.8738, with a controller given by:

$$\frac{U(s^*)}{E(s^*)} = \frac{(s^* + 272.66)}{(s^* + 180.67)} \frac{(s^* + 10)}{(s^* + 10.033)} \frac{(s^{2} * + 2.2398 s^* + 0.845)}{(s^{2} * + 9.4986 s^* + 33.823)} \cdot \frac{(s^* + .14646)}{(s^* + 1.2783)} \frac{(s^* + 1.0009\text{E-}4)}{(s^* + 4.7767E-2)} \frac{(s^* + 0.9991E-4)}{(s^{2} * + 5.4E-3 s^* + 7.29E-6)} \tag{23}$$

where *E(s*)* is the error between the reference signal and previewed feedback. Examination reveals that this controller is acting to perform to pseudo-inversion of the plant and control weightings, a fact that will sharply limit the performance due to the uncertainty of the system. The H-infinity controller synthesis with the previous weights

achieved the following loop shapes, which show that all specifications were met:

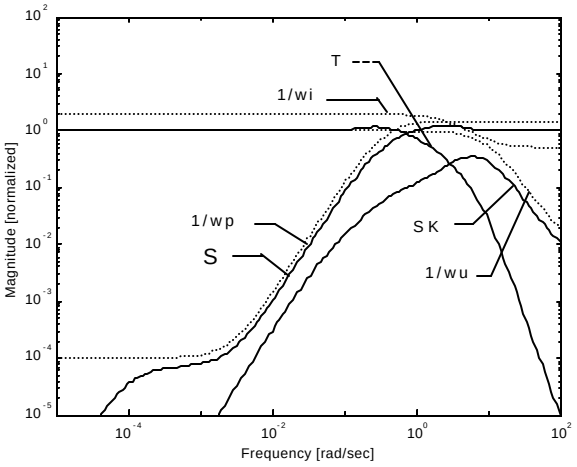

Fig. 4: Controller loop shapes

Note that the above controller is designed in nondimensional time and space. For implementation in 'true' space, one must multiply by the correct time and spatial factors. In the vehicle case, the spatial correction is obtained from (14) and is a constant:

$$Correction = \frac{u^*_{max}}{e^*_{max} \cdot L} \cdot$$

The temporal correction is obtained by dividing all pole locations by the time factor **S** used in Equation (7).

Experimental testing of this H-infinity controller was conducted in both simulation and experimental platforms. The simulation was necessary to represent the full possible range of vehicle plants, while the experimental vehicle is used to introduce real-world plant variations including nonlinearities, unmodeled dynamics, and disturbances that are otherwise ignored in a simulation study. For the experimental vehicle to operate at a fixed Π_3 value of 0.5, it was driven at a speed of 3.0 m/s. This speed approximates an 'average' full-sized vehicle at a speed of 50 mph.

The vehicle responses from the experimental vehicle are shown in Fig. 7 above as the vehicle attempts to track a square wave. The H-infinity controller is very underdamped and low-gain, a result that should be expected in consideration of essentially single-state feedback combined with severe robustness constraints. However, there was no system identification outside of measurement of basic parameters: vehicle mass, vehicle length, vehicle velocity, and tire cornering stiffness. The controller was designed to be robust enough to operate nearly any vehicle, so the effectiveness of the controller on this arbitrary vehicle without identification is not surprising. Such a result greatly validates a methodology of utilizing nondimensional robustness measures to achieve very general controllers.

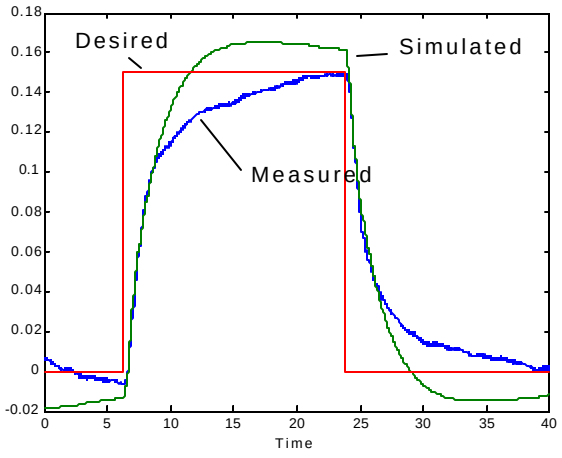

Fig. 5: Experimental closed loop step responses

In terms of the tuning variables for the controller, the key factor limiting the performance is the choice of performance bandwidth, w_{BP}, in Equation (21). Improved bandwidth can be obtained, but significant improvement is obtained only by violating the norm criteria of Equation (20). For instance, increasing w_{BP} to 0.5 gives a gamma value of 1.1, a value of w_{BP} of 1 gives a gamma of 1.5. Further, plots of the controller loop shapes for this w_{BP} show possible violation of robustness constraints. This classic tradeoff between robustness and performance is well known, and the exact choice of values depends on the intent of the control designer.

5. Extensions to Velocity Scheduling

The previous result was presented for a fixed Π_3 value, which necessarily corresponds to a fixed velocity and cornering stiffness (representative of fixed road friction). In the case where some type of velocity gain scheduling is desired, note that velocity enters the nondimensional form of the bicycle model through the parameters of Π_3 and Π_4. For a particular vehicle, $\mathbf{V_i}$, we may fix the ratio of these two parameters, so that Π_4 is a constant function of Π_3 without loss of generality. Because friction and velocity enter the dynamic equations through the same parameter, we conclude that velocity gain scheduling must be used cautiously, because appropriate scheduling of the Π_3 requires very good knowledge of the road friction. The duality of friction scheduling and velocity scheduling is discussed in more detail in [3].

At each velocity, the controller must still be robust to model variation, and therefore bounds on the model uncertainty must be recalculated at each operating condition. With a fixed preview of 2 seconds, the upper bounds on uncertainty were calculated for many Π_3 values, and are shown in the figure below:

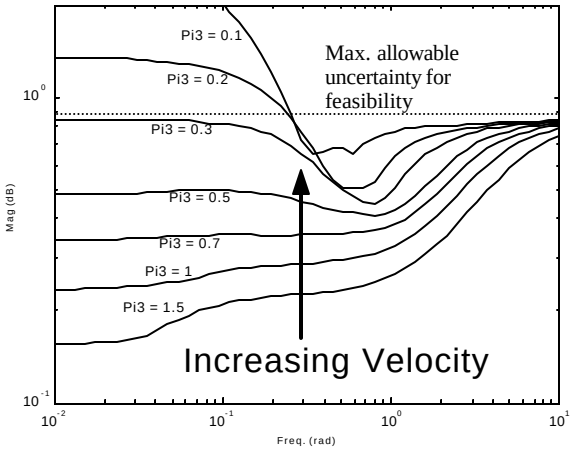

Fig. 6: Effect of velocity on uncertainty

Because the uncertainty cannot be larger than unity, there is clearly some limiting Π_3 value below which robust vehicle lateral control is not achievable due to increasing system uncertainty. The limiting case corresponds to:

$$\Pi_{3,CRITICAL} \approx 0.27 \cdot \tag{24}$$

From this information and Equation (1), one may back-calculate the speed/cornering-stiffness relationship at which generalized robust control is no longer feasible, which we call the critical speed for robustness:

$$U_{C,R} \approx \sqrt{\frac{L \cdot Ca\, f}{0.27 \cdot m}}. \tag{25}$$

Note that the vehicle mass, *m*, and length, *L*, are easy to measure and remain approximately fixed for a given vehicle. For the vehicles in the database, **V**, the value of $U_{C,R}$ ranges between extremes of 15 and 45 m/s (30 to 100 mph) because of differences in reported road friction. The majority of vehicles in **V** have critical robustness speeds of 25 m/s (about 55 mph).

The critical robustness speed has interesting implications for vehicle control, as other researchers have pointed out that significant modifications to control approaches are needed to achieve high-speed lateral control [10]. In the MIMO control case, the limiting case of Equation (24) could be calculated using the maximum singular values of the uncertainty model. In either case, we must conclude that severe limits exist to robust, high-speed vehicle control algorithms.

6. Conclusions

The controller presented in this work addressed controller robustness in a generalized nondimensional framework that brings insight to the feasibility of a robust controller design. By parameterizing plant uncertainty nondimensionally, normal distributions were obtained of the plant parameters that defined an average plant. Measured differences between a vehicle database and an average plant motivated a multiplicative uncertainty description.

An H-infinity methodology is then presented that utilizes a stacked sensitivity approach. While this approach achieves robust control, it is only by sacrificing performance. Discussion is given to extensions of the work to velocity scheduling, and a limiting speed/friction relationship is encountered that defines operating regions where robust control is and is not achievable.

References

[1] J. Ackermann, "1996 Bode Prize Lecture: Robust Control Prevents Car Skidding," in *IEEE Conference on Decision and Control, June 1996, Reprinted in IEEE Control Systems Magazine, June 1997*, 1996, pp. 23-31.

[2] Tagawa, T., e.a. "A Robust Active Front Wheel Steering System Considering the Limits of Vehicle Lateral Force," presented at Proceedings of AVEC'96, Aachen, 1996.

[3] S. Brennan and A. Alleyne, "Robust Stabilization of a Generalized Vehicle, a Nondimensional Approach," presented at 5th International Symposium on Advanced Vehicle Control (AVEC), University of Michigan, Ann-Arbor, 2000.

[4] S. Horiuchi, N. Yuhara, and A. Takei, "Two Degree of Freedom H-infinity Controller Synthesis for Active Four Wheel Steering Vehicles," *Vehicle System Dynamics Supplement*, vol. 25, pp. 275-292, 1996.

[5] E. Ono, K. Takanami, N. Iwama, Y. Hayashi, Y. Hirano, and Y. Satoh, "Vehicle Integrated Control for Steering and Traction Systems by Mu-Synthesis," *Automatica*, vol. 30, pp. 1639-1647, 1994.

[6] J. Sun, A. W. Olbrot, and M. P. Polis, "Robust Stabilizations and Robust Performance Using Model Reference Control and Modeling Error Compensation," *IEEE Transactions on Automatic Control*, vol. 39, pp. 630-635, 1994.

[7] E. Buckingham, "On Physically Similar Systems; Illustrations of the use of dimensional equations," *Physical Review*, vol. 4, pp. 345-376, 1914.

[8] S. Brennan and A. Alleyne, "Using a Scale Testbed: Controller Design and Evaluation," in *IEEE Control Systems Magazine*, vol. 21, 2001, pp. 15-26.

[9] A. Alleyne, "A Comparison of Alternative Obstacle Avoidance Strategies for Vehicle Control," *Vehicle System Dynamics*, vol. 27, pp. 371-392, 1997.

[10] S. Patwardhan, H.-S. Tan, and J. Guldner, "A General Framework for Automatic Steering Control: System Analysis," presented at Proceedings of the American Control Conference, Albuquerque, NM, 1997.

[11] H. Peng and M. Tomizuka, "Preview Control for Vehicle Lateral Guidance in Highway Automation," *ASME Journal of Dynamic Systems, Measurement and Control*, vol. 115, pp. 679-686, 1993.

[12] J. Guldner, H. S. Tan, and S. Patwardhan, "Analysis of Automatic Steering Control for Highway Vehicles with Look-Down Lateral Reference Systems," *Vehicle System Dynamics*, vol. 26, pp. 243-269, 1996.

[13] S. Skogestad and I. Postlethwaite, *Multivariable Feedback Control, Analysis and Design*. Chichester: Wiley, 1996.